nature medicine

Methylglyoxal modification of $Na_V1.8$ facilitates nociceptive neuron firing and causes hyperalgesia in diabetic neuropathy

Angelika Bierhaus[1,20], Thomas Fleming[1,20], Stoyan Stoyanov[1], Andreas Leffler[2,3], Alexandru Babes[4,5], Cristian Neacsu[5], Susanne K Sauer[4], Mirjam Eberhardt[4], Martina Schnölzer[6], Felix Lasischka[7], Winfried L Neuhuber[4], Tatjana I Kichko[4], Ilze Konrade[1,8], Ralf Elvert[9], Walter Mier[10], Valdis Pirags[11], Ivan K Lukic[1,12], Michael Morcos[1], Thomas Dehmer[13], Naila Rabbani[14], Paul J Thornalley[14], Diane Edelstein[15], Carla Nau[3], Josephine Forbes[16], Per M Humpert[1], Markus Schwaninger[17], Dan Ziegler[18], David M Stern[19], Mark E Cooper[16], Uwe Haberkorn[10], Michael Brownlee[15,20], Peter W Reeh[4] & Peter P Nawroth[1]

This study establishes a mechanism for metabolic hyperalgesia based on the glycolytic metabolite methylglyoxal. We found that concentrations of plasma methylglyoxal above 600 nM discriminate between diabetes-affected individuals with pain and those without pain. Methylglyoxal depolarizes sensory neurons and induces post-translational modifications of the voltage-gated sodium channel $Na_V1.8$, which are associated with increased electrical excitability and facilitated firing of nociceptive neurons, whereas it promotes the slow inactivation of $Na_V1.7$. In mice, treatment with methylglyoxal reduces nerve conduction velocity, facilitates neurosecretion of calcitonin gene-related peptide, increases cyclooxygenase-2 (COX-2) expression and evokes thermal and mechanical hyperalgesia. This hyperalgesia is reflected by increased blood flow in brain regions that are involved in pain processing. We also found similar changes in streptozotocin-induced and genetic mouse models of diabetes but not in $Na_V1.8$ knockout (*Scn10*$^{-/-}$) mice. Several strategies that include a methylglyoxal scavenger are effective in reducing methylglyoxal- and diabetes-induced hyperalgesia. This previously undescribed concept of metabolically driven hyperalgesia provides a new basis for the design of therapeutic interventions for painful diabetic neuropathy.

Pain and hyperalgesia are key danger signals that are evoked by physical insults, noxious chemicals and inflammation. Such danger signals are also present in patients with diabetic neuropathy despite losses in sensory and autonomic functions in these individuals. Whereas the molecular mechanisms underlying inflammatory hyperalgesia are increasingly being unraveled, there is currently only a vague understanding of the mechanisms causing neuropathic pain in metabolic diseases such as diabetes[1]. In general, hyperglycemia has been emphasized as a major risk factor in these diseases; however, normalization of glucose concentrations has shown little benefit in affected individuals[1–3].

Elevated glucose concentrations lead to increased formation of the highly reactive dicarbonyl metabolite methylglyoxal[4], which is metabolized by glyoxalase 1 (GLO1) and GLO2 to the end product D-lactate[4–7]. As peripheral nerves have low GLO1 activity[8,9], it has been reasoned that they might be particularly vulnerable to methylglyoxal accumulation. As has been shown in the model organism *Caenorhabditis elegans*, the glyoxalase system is essential for neuronal integrity[10]. A recent study comparing the expression of GLO1 in various inbred mouse strains showed a negative correlation between GLO1 expression and mechanical hyperalgesia, implying that the balance between methylglyoxal and GLO1 might directly modulate pain perception[9].

Increased electrical excitability seems to be the underlying cause of the generation of orthotopic or ectopic impulses in experimental rat

[1]Department of Medicine I and Clinical Chemistry, University Hospital Heidelberg, Heidelberg, Germany. [2]Department of Anesthesiology and Intensive Care, Hannover Medical School, Hannover, Germany. [3]Department of Anesthesiology, Friedrich-Alexander-University Erlangen-Nuremberg, Erlangen, Germany. [4]Institute of Physiology and Pathophysiology, Friedrich-Alexander-University Erlangen-Nuremberg, Erlangen, Germany. [5]Department of Physiology and Biophysics, Faculty of Biology, University of Bucharest, Bucharest, Romania. [6]Functional Proteome Analysis B100, Core Facility Protein Analysis W120, German Cancer Research Center, Heidelberg, Germany. [7]Institute of Pathology, University Hospital Heidelberg, Heidelberg, Germany. [8]Stradins University, Riga Eastern Clinical University Hospital, Riga, Latvia. [9]Sanofi-Aventis Deutschland, Frankfurt, Germany. [10]Department of Nuclear Medicine, University Hospital Heidelberg, Heidelberg, Germany. [11]University of Latvia, Pauls Stradins Clinical University Hospital, Riga, Latvia. [12]Biosistemi d.o.o., Zagreb, Croatia. [13]Zentrum für Psychiatrie Südwürttemberg, Zwiefalten, Germany. [14]Warwick Medical School, Clinical Sciences Research Institute, University of Warwick, University Hospital, Coventry, UK. [15]Albert Einstein College of Medicine, Bronx, New York, USA. [16]Baker International Diabetes Institute, Heart and Diabetes Institute, Melbourne, Victoria, Australia. [17]Institute for Experimental und Clinical Pharmacology and Toxicology, University of Lübeck, Lübeck, Germany. [18]Institute for Clinical Diabetology, German Diabetes Center at the Heinrich Heine University Leibniz Center For Diabetes Research, Düsseldorf, Germany. [19]University of Tennessee College of Medicine, Memphis, Tennessee, USA. [20]These authors contributed equally to this work. Correspondence should be addressed to P.P.N. (peter.nawroth@med.uni-heidelberg.de).

Received 30 November 2011; accepted 22 March 2012; published online 13 May 2012; doi:10.1038/nm.2750

and human diabetic neuropathy[11,12]. Reduced potassium conductance and reduced Na^+/K^+ ATPase activity in diabetic nerves have been proposed as possible causes of increased excitability[12–14], but changes in neuronal voltage-gated sodium channels (VGSCs), which trigger, shape and propagate action potentials, could also directly explain the increased excitability. The effect of diabetes on VGSC gene expression has yielded results with some discrepancies that cannot account for the coexistence of positive and negative symptoms in diabetic neuropathy[15–17]. One particular VGSC, tetrodotoxin-resistant (TTXr) $Na_v1.8$, is exclusively expressed in pain-signaling neurons or nociceptors[18,19]; however, $Na_v1.8$ transcription and expression are decreased in diabetic rats[15,16] with increased TTXr sodium currents[16–20]. These seemingly contradictory findings led to a hypothesis that post-translational modifications in $Na_v1.8$ by methylglyoxal could increase either voltage sensitivity or functional channel availability, causing the hyperexcitability that is responsible for diabetic hyperalgesia and spontaneous pain.

In this study, we show that increased concentrations of methylglyoxal may account for metabolic hyperalgesia. The link between hyperalgesia and methylglyoxal is provided by nonenzymatic modifications of $Na_v1.8$, which, in turn, modify its function. Our data provide evidence for a previously unidentified pathway in which methylglyoxal directly induces hyperalgesia and may provide new therapeutic options for the treatment of painful metabolic neuropathy.

RESULTS

We found that plasma methylglyoxal discriminated patients with type 2 diabetes from healthy controls (**Fig. 1a**). Assessment of pain, determined by self report in the foot and graded on a ten point numerical scale, showed that the patients with diabetes could be subdivided into two groups: those with no pain and those with pain. Patients were considered to have pain when they reported more than seven points on the numeric scale. The mean pain scores for the two groups were 1.7 ± 1.2 and 7.7 ± 1.0 (mean ± s.e.m.) (for those with no pain and those with pain, respectively). Patients with pain also reported significantly more burning sensations and had a trend towards increased dysesthesia (**Fig. 1b**). The groups did not differ significantly in their neuropathy deficit score or in a range of metabolic variables (**Supplementary Table 1**). We subsequently found that diabetes-affected individuals with pain had significantly higher concentrations of plasma methylglyoxal (≥600 nM) compared to either healthy controls or diabetes-affected individuals with no pain (**Fig. 1a**), which is consistent with recent observations in patients with type 1 diabetes[21]. To establish whether these elevated concentrations of methylglyoxal could affect neuronal function, we exposed cultured mouse dorsal root ganglion (DRG) neurons from healthy wild-type (WT) mice to plasma from either healthy controls or diabetes-affected individuals with or without pain. We determined the induction of COX-2 as an indirect readout for altered neuronal function. Plasma from patients with pain induced significantly more COX-2 transcription in the neurons than plasma from controls or patients with no pain (**Fig. 1c**). Treatment with trypsin of the plasma from patients with pain did not prevent COX-2 expression in the neurons. The supplementation with exogenous methylglyoxal of plasma isolated from individuals with diabetes without pain to elevate the concentrations to those observed in patients with pain (≥600 nM) resulted in further increases in COX-2 transcription in the neuron (**Supplementary Fig. 1b**). As the activity of GLO1 is low in peripheral nerves and is even lower in peripheral nerves of diabetic mice[8,9] (**Fig. 1d**), we reasoned that neurons might be particularly likely to accumulate methylglyoxal.

Inhibition of GLO1 (ref. 22) by the cell-permeable inhibitor s-p-bromobenzylglutathione cyclopentyl diester in nondiabetic WT mice resulted in profound thermal hyperalgesia when the methylglyoxal plasma concentrations exceeded 600 nM (**Fig. 2a**). WT mice in which we induced diabetes with streptozotocin (STZ-induced diabetic WT mice) (8-week duration) showed a pronounced latency reduction in noxious heat withdrawal (**Fig. 2b**). Nondiabetic GLO1 knockdown ($Glo1^{-/+}$) mice[23] showed an equally pronounced latency reduction compared to STZ-induced diabetic WT mice. STZ-induction of diabetes in $Glo1^{-/+}$ mice (8-week

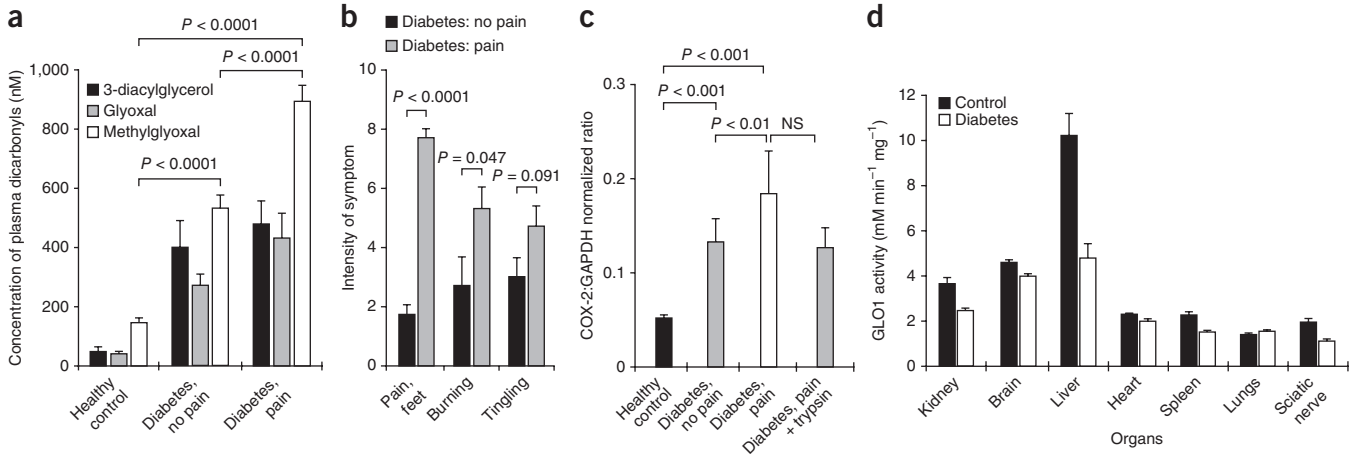

Figure 1 Methylglyoxal and pain in individuals with diabetes. (**a**) Plasma dicarbonyl concentrations in the patients with type 2 diabetes characterized in **Supplementary Table 1** with and without pain. Data represent the mean ± s.e.m. $n = 10$ patients per group (comparisons were made using analysis of variance (ANOVA)). (**b**) Intensity of neuropathy symptoms in the studied diabetes-affected individuals with and without pain as assessed by self report in the foot and graded on a ten point numerical scale. Data represent the mean ± s.e.m. $n = 10$ patients per group (unpaired, two-tailed Student's t test). (**c**) Quantification of COX-2 mRNA expression in DRGs isolated from healthy C57BL/6 WT mice treated with heat-inactivated plasma from healthy subjects (controls) or diabetes-affected individuals with and without pain. Where indicated, plasma samples from patients with diabetes and pain were pretreated with trypsin and neutralized using Soybean inhibitor. Data represent the mean of three independent experiments performed in triplicates ± s.d. $n = 3$ mice per group. GAPDH, glyceraldehyde-3-phosphate dehydrogenase; NS, not significant (unpaired, two-tailed Student's t test). (**d**) Organ survey for GLO1 activity in tissue extracts from healthy and STZ-induced diabetic WT mice. Data represent the mean ± s.d. $n = 10$ mice per group.

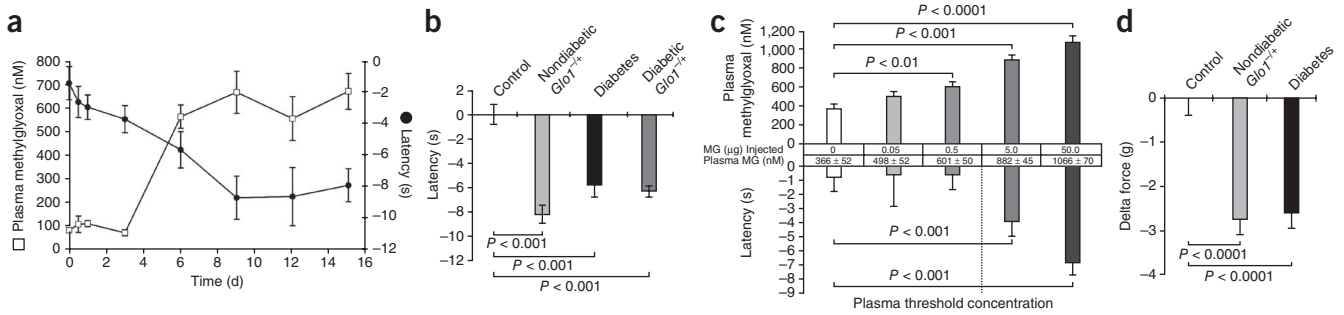

Figure 2 Exogenous methylglyoxal (MG) and STZ-induced diabetes induce thermal hyperalgesia. (**a**) Inhibition of GLO1 by the cell-permeable inhibitor S-p-bromobenzylglutathione cyclopentyl diester in healthy WT mice. Hyperalgesia was assessed by Hot Plate assay at day 0 before application of the inhibitor. Consecutive assessments of methylglyoxal plasma concentrations and thermal hyperalgesia were made at selected time points. Data represent the mean ± s.d. $n = 3$ mice per time point. (**b**) Thermal hyperalgesia in nondiabetic WT and GLO1 knockdown ($Glo1^{-/+}$) mice and diabetic WT mice 8 weeks after STZ-induced diabetes, as measured by Hot Plate assay. Data represent the mean ± s.e.m. $n = 20$–25 mice per group (ANOVA). (**c**) Responses to heat stimulation by Hot Plate assay in methylglyoxal-treated WT mice. Plasma was isolated for methylglyoxal anaylsis by HPLC. Data represent the mean ± s.d. ($n = 3$ mice per group) for methylglyoxal plasma concentrations and the mean ± s.e.m. ($n = 10$ mice per group) for hyperalgesia determination (ANOVA). (**d**) Mechanical hyperalgesia (tactile allodynia) in nondiabetic WT and $Glo1^{-/+}$ mice and STZ-induced diabetic WT mice, as determined by Frey filament test. Data represent the mean ± s.e.m. $n = 10$ mice per group (ANOVA).

duration) had no further sensitizing effect. Systemic administration of methylglyoxal resulted in an increase in methylglyoxal plasma concentrations and a dose-dependent thermal hyperalgesia response within 3 h of administration (**Fig. 2c** and **Supplementary Fig. 2a–c**). The methylglyoxal-induced sensitization to noxious heat was obscured when the hot plate temperature applied was 55 °C rather than 50 °C, implying that methylglyoxal lowered the heat threshold but did not disable the nocifensive response (**Supplementary Fig. 2d**). Diabetes, GLO1 deficiency and systemic methylglyoxal administration also induced pronounced mechanical hyperalgesia (**Fig. 2d** and **Supplementary Fig. 2e**).

Increased concentrations of methylglyoxal in diabetic mice are caused, in part, by reduced GLO1 transcription, expression and activity (**Supplementary Fig. 3a–c**). We achieved fully comparable results to those in the STZ-induced diabetic WT mice when we studied methylglyoxal concentrations in spontaneously diabetic BKS db/db mice[24] (**Supplementary Fig. 4**). The observed robust thermal and mechanical hyperalgesia in the STZ-induced diabetic WT mice after 8 weeks of hyperglycemia occurs at a time in which nonspecific STZ-derived inflammatory processes have dispersed[24] and no gross morphological changes in peripheral nerves are present on the ultrastructural level (data not shown). In STZ-induced diabetic WT mice, we found an induction of COX-2 immunoreactivity in the hindpaw epidermis (**Supplementary Fig. 3d**), which is consistent with the COX-2–inducing effect of patient plasma on DRG neurons (**Fig. 1c** and **Supplementary Fig. 1b**) and with excessive prostaglandin formation in diabetic rat skin[18]. Thus, non-neuronal and neuronal induction of COX-2, a marker of cellular activation and a producer of sensitizing eicosanoids[18], may be driven by increased concentrations of methylglyoxal.

Overexpression of GLO1 in STZ-induced diabetic WT mice (8-week duration) by somatic gene transfer resulted in an increase in sciatic GLO1 activity, decreased plasma methylglyoxal concentrations and reduced thermal hyperalgesia (**Fig. 3a–c**). This effect

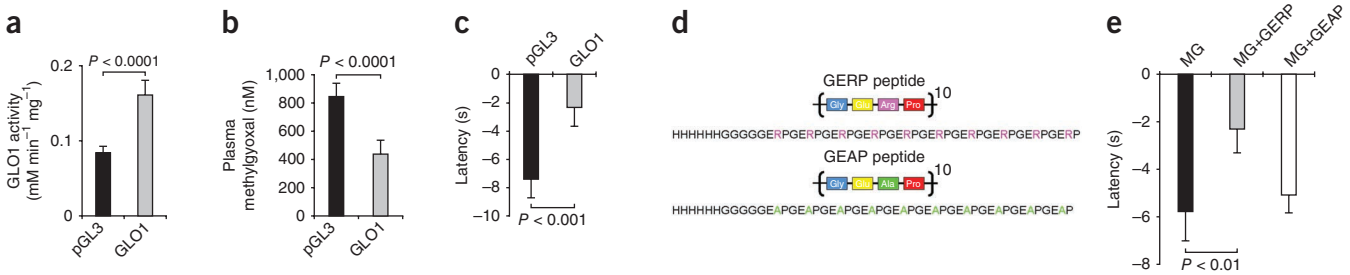

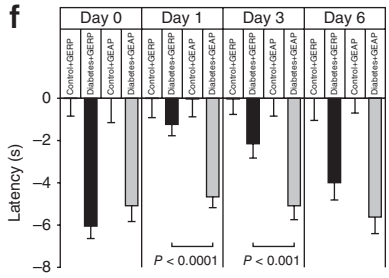

Figure 3 Overexpressing GLO1 or scavenging methylglyoxal by a synthetic peptide reduces thermal hyperalgesia in methylglyoxal-treated and diabetic mice. STZ-induced diabetic mice were treated every 2 d for 10 d with either GLO1-overexpressing vector (GLO1) or control vector (pGL3). (**a**) GLO1 activity in sciatic nerve tissue. Data represent the mean ± s.d. $n = 5$ mice per group (unpaired, two-tailed Student's t test). (**b**) Plasma methylglyoxal concentrations. Data represent the mean ± s.e.m. $n = 10$ mice per group (unpaired, two-tailed Student's t test). (**c**) Thermal hyperalgesia after 10 d of treatment with the GLO1-overexpressing vector by intravenous injection into the tail vein. Data represent the mean ± s.e.m. $n = 10$ mice per group (unpaired, two-tailed Student's t test). (**d**) A synthetic peptide, $GERP_{10}$ (GERP), was designed containing ten arginine residues per molecule to act as an effective *in vivo* scavenger of methylglyoxal. The peptide $GEAP_{10}$ (GEAP) served as an arginine-free control. (**e**) Healthy WT mice were injected with GERP or the control peptide GEAP before injection of methylglyoxal. Hyperalgesia was assessed 3 h after methylglyoxal injection by Hot Plate assay. Data represent the mean ± s.e.m. $n = 10$ mice per group (ANOVA). (**f**) The effects of GERP and GEAP on diabetes-induced hyperalgesia in STZ-induced diabetic WT mice. Data represent the mean ± s.e.m. $n = 10$ mice per group (ANOVA).

was independent of the pathway involving the advanced glycation endproducts (AGEs) and their receptor (the AGE-RAGE pathway), as systemic administration of carboxymethyl-lysine (800 nM, 3 h) did not induce thermal hyperalgesia (data not shown). Further, injection of methylglyoxal (5 µg, 3 h) into RAGE knockout (*Ager*$^{-/-}$) mice caused thermal hyperalgesia that was indistinguishable from that observed in the STZ-induced diabetic WT mice (data not shown). In contrast, treatment with either aminoguanidine, a scavenger of free methylglyoxal, or alagebrium (ALT-711), a compound that breaks AGE-derived crosslinks in proteins, inhibited methylglyoxal-induced hyperalgesia in methylglyoxal-treated WT mice (**Supplementary Fig. 5**), implying that *de novo* post-translational modifications of membrane proteins are responsible for the increased sensitivity and excitability of primary sensory neurons in these mice. To scavenge excessive concentrations of methylglyoxal *in vivo*, we designed an arginine-rich peptide ($GERP_{10}$) and a control peptide devoid of arginine ($GEAP_{10}$) (**Fig. 3d**). Systemic administration of $GERP_{10}$ reduced thermal hyperalgesia in both methylglyoxal-treated WT mice (**Fig. 3e**) and STZ-induced diabetic WT mice (**Fig. 3f**), with a half-life of approximately 80 h, whereas systemic administration of $GEAP_{10}$ had no effect in either of these groups.

To identify a possible protein target of post-translational modifications by methylglyoxal, we determined the expression of VGSCs in DRGs. Transient receptor potential V1 (TRPV1) and COX-2 expression served as positive controls for DRG expression[25,26]. Expression of $Na_v1.7$ and $Na_v1.9$ did not differ between the DRGs from nondiabetic WT and STZ-induced diabetic WT mice, whereas $Na_v1.8$ expression was slightly lower, but not significantly lower, in the STZ-induced diabetic WT mice compared to the nondiabetic WT mice[15,16] (**Fig. 4a**). Methylglyoxal-induced modifications of arginine residue(s) within the DIII-DIV linker of $Na_v1.8$ (comprising its inactivation gate) might alter the gating properties of $Na_v1.8$. Immunoprecipitations of DRGs isolated from rats treated with methylglyoxal, healthy WT mice treated with methylglyoxal, STZ-induced diabetic WT mice (8-week duration) and healthy *Glo1*$^{-/+}$ mice showed that modifications of $Na_v1.8$ by methylglyoxal were increased in the presence of

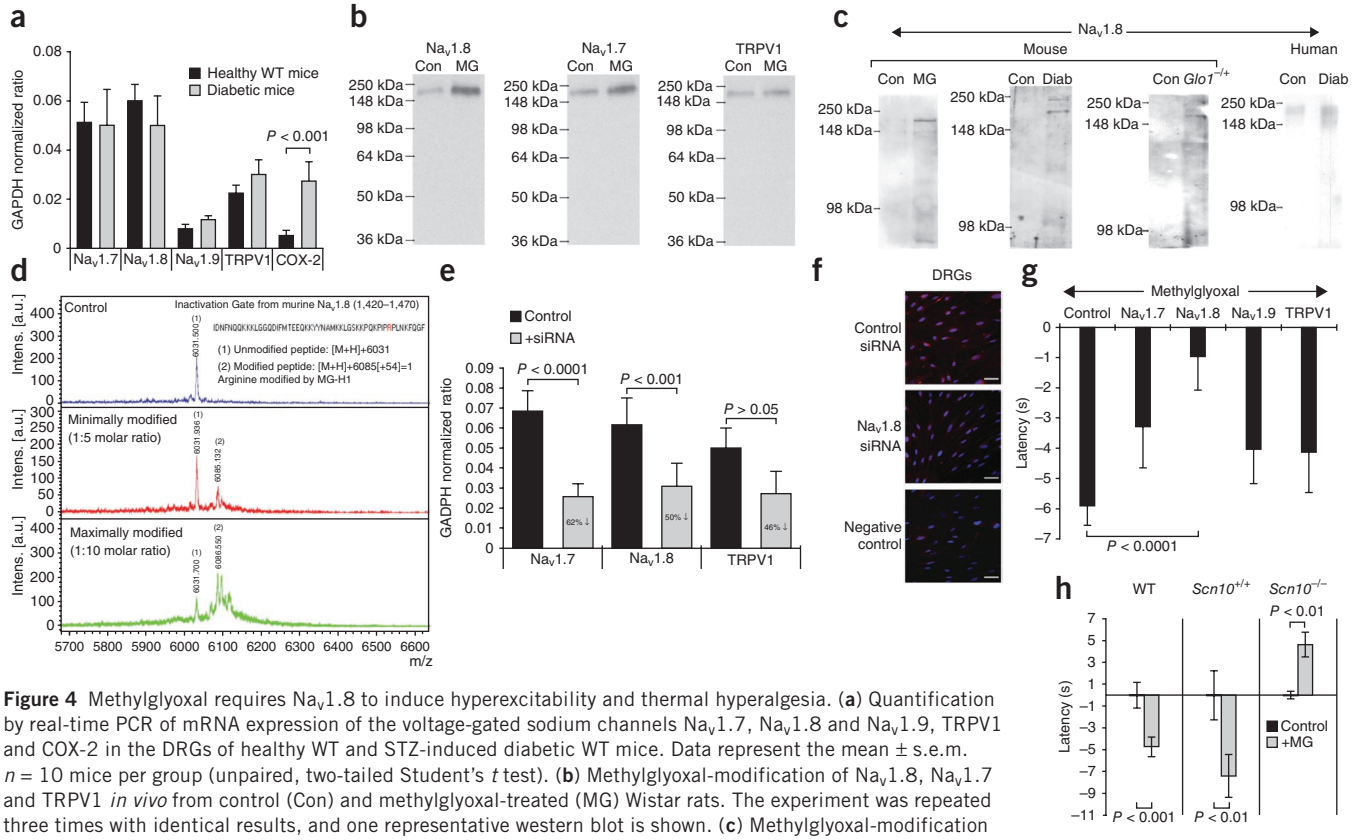

Figure 4 Methylglyoxal requires $Na_v1.8$ to induce hyperexcitability and thermal hyperalgesia. (**a**) Quantification by real-time PCR of mRNA expression of the voltage-gated sodium channels $Na_v1.7$, $Na_v1.8$ and $Na_v1.9$, TRPV1 and COX-2 in the DRGs of healthy WT and STZ-induced diabetic WT mice. Data represent the mean ± s.e.m. $n = 10$ mice per group (unpaired, two-tailed Student's t test). (**b**) Methylglyoxal-modification of $Na_v1.8$, $Na_v1.7$ and TRPV1 *in vivo* from control (Con) and methylglyoxal-treated (MG) Wistar rats. The experiment was repeated three times with identical results, and one representative western blot is shown. (**c**) Methylglyoxal-modification of $Na_v1.8$ *in vivo* from control healthy (Con), methylglyoxal-treated (MG), STZ-induced diabetic (Diab) and healthy *Glo1*$^{-/+}$ (*Glo1*$^{-/+}$) mice. For each group, DRGs were pooled from at least ten mice. Human sciatic nerve material was obtained from biopsies from patients with (Diab) or without diabetes (Con). The experiment was repeated three times with identical results, and one representative western blot is shown. (**d**) Methylglyoxal directly binds to the arginine residue in the $Na_v1.8$ activation gate. The DIII-DIV linker of murine $Na_v1.8$ was synthesized and incubated without (control) or with methylglyoxal in an either 1:5 (minimally modified) or 1:10 (maximally modified) molar ratio[35]. A single peak with $[M+H]^+$ 6,031 (peak 1) was observed under control conditions. Under both minimal and maximal conditions, a modified peptide was observed with a mass difference of 54 Da (peak 2; 6,085 Da versus 6,031 Da), which corresponds to the modification of the arginine residue at position 43 of the peptide by methylglyoxal to form the hydroimidazolone MG-H1. (**e**) Effects of *in vivo* siRNA treatment on the expression of $Na_v1.7$, $Na_v1.8$ and TRPV1 in healthy WT DRGs, as determined by real-time PCR. Data represent the mean ± s.d. $n = 3$ mice per group (unpaired, two-tailed Student's t test). (**f**) Effects of *in vivo* siRNA treatment for $Na_v1.8$ in healthy WT DRGs, as determined by immunocytochemistry. The experiment was repeated three times with identical results, and one representative staining is shown. Scale bars, 50 µm. (**g**) Effect of *in vivo* siRNA treatment for $Na_v1.7$, $Na_v1.8$ and $Na_v1.9$ on methylglyoxal-induced thermal hyperalgesia in mice. Data represent the mean ± s.e.m. $n = 10$ mice per group (unpaired, two-tailed Student's t test). (**h**) Effect of exogenous methylglyoxal on hyperalgesia in healthy WT mice, WT littermates of the $Na_v1.8$ knockout mice (*Scn10a*$^{+/+}$) and $Na_v1.8$ knockout mice (*Scn10a*$^{-/-}$). Data represent the mean ± s.d. $n = 5$ or 6 mice per group (unpaired, two-tailed Student's t test).

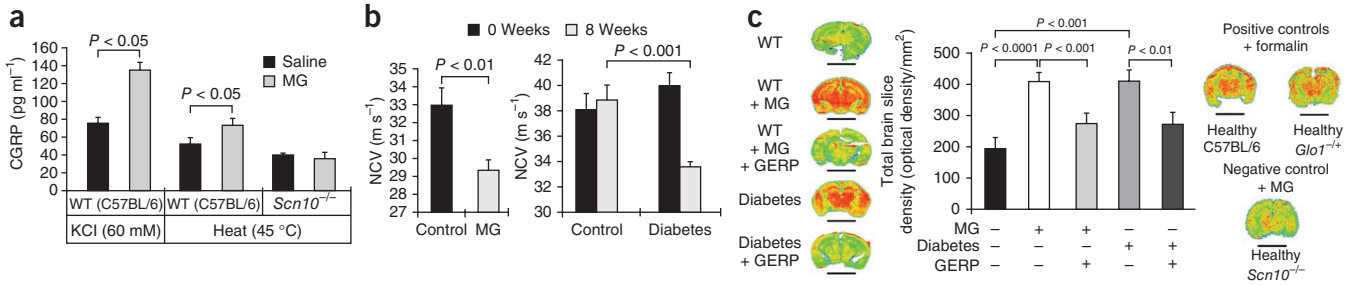

Figure 5 Methylglyoxal causes a cascade of neurochemical changes and activates brain regions involved in pain processing. (**a**) Effect of systemic methylglyoxal treatment on KCl- and heat-induced CGRP release from isolated hindpaw skin of healthy WT and $Na_v1.8$ knockout (*Scn10a*$^{-/-}$) mice after systemic methylglyoxal pretreatment. Data represent the mean ± s.e.m (two-tailed Student's *t* test). (**b**) Maximal dorsal tail NCV determined in healthy WT mice untreated (control) or pretreated with methylglyoxal ($n = 7$ mice in each group) and in healthy WT (control) and STZ-induced diabetic WT mice (diabetes) ($n = 12$ mice in each group). Data represent the mean ± s.d. (unpaired, two-tailed Student's *t* test). (**c**) CBF changes show increased brain activity. Sample colorized coronal sections showing differences in brain activation after heat stimulation; increased CBF is indicated in red. Each image is taken from a single brain section in the individual mice. Data represent the mean ± s.d., $n = 4$ mice per group (ANOVA), and one representative brain section is shown for each condition. Scale bars, 50 mm.

methylglyoxal, diabetes and the deficit in GLO1 (**Fig. 4b**). Further, in sciatic nerve tissue isolated from patients with or without diabetes who had amputations resulting from peripheral artery disease, we observed that the patients with diabetes had substantially more modifications of $Na_v1.8$ by methylglyoxal than the patients without diabetes (**Fig. 4c**). Incubation of a peptide, comprising the inactivation gate of $Na_v1.8$, with methylglyoxal followed by a mass spectrometry analysis confirmed that methylglyoxal binds to the arginine residue within the $Na_v1.8$ inactivation gate sequence (**Fig. 4d**). When we incubated plasma from diabetes-affected individuals with the peptide, peptide mapping confirmed methylglyoxal binding to the arginine residue in the $Na_v1.8$ inactivation gate (**Supplementary Fig. 6**).

Systemic treatment of WT mice with siRNA targeting $Na_v1.7$, $Na_v1.8$ or TRPV1 resulted in a significant inhibition of the respective mRNA (**Fig. 4e**,**f**). The $Na_v1.8$ knockdown was paralleled a by loss of methylglyoxal-induced thermal hyperalgesia (**Fig. 4g** and **Supplementary Fig. 7a**). In addition, the $Na_v1.8$ knockout mice were not only protected from methylglyoxal-induced hyperalgesia but actually showed hypoalgesia; we observed wild-type littermates of the $NA_V1.8$ knockout mice (*Scn10a*$^{+/+}$) to have a similar methylglyoxal-induced hyperalgesia to the C57BL/6 mice used throughout the study (**Fig. 4h** and **Supplementary Fig. 7b**).

We also found that *in vivo* pretreatment with methylglyoxal of healthy WT or $Na_v1.8$ knockout mice facilitated the potassium-induced and noxious-heat–induced release of the proinflammatory neuropeptide calcitonin gene-related peptide (CGRP) from cutaneous nociceptors *in vitro* (**Fig. 5a**), indicating increased responsiveness to both nonspecific and heat-transduced membrane depolarization of the skin nerve endings as a result of the pretreatment with methylglyoxal. Sensitization to heat, but not the heat response itself, was absent in skin flaps from the methylglyoxal-pretreated $Na_v1.8$ knockout mice. Methylglyoxal pretreatment and diabetes both significantly reduced the maximal tail nerve conduction velocity (NCV) (**Fig. 5b**) despite the absence of overt morphological changes (data not shown), a preclinical signature of the imminent large-fiber neuropathy.

We next determined the cerebral blood flow (CBF) changes in the pain-processing regions of the brain[27] in mice we stimulated with laser-evoked noxious heat. We visualized the blood flow distribution in these mice using pseudocolored frontal brain sections showing the resting and activated brain regions (**Fig. 5c**). We found increased heat responses in healthy WT mice pretreated with methylglyoxal and in STZ-induced diabetic WT mice compared to healthy WT mice, whereas the methylglyoxal-scavenging peptide $GERP_{10}$ showed an antihyperalgesic effect in the healthy WT methylglyoxal-pretreated and STZ-induced diabetic WT mice. $Na_v1.8$ knockout mice did not have an enhanced heat response after methylglyoxal pretreatment. Formalin injection in healthy WT mice, to induce pain without radiant heat, or healthy *Glo1*$^{-/+}$ mice plus heat stimulation showed an enhanced cerebral blood flow comparable to that in methylglyoxal-pretreated or STZ-induced diabetic WT mice. Notably, the areas of increased blood flow in all mouse brains studied (bregma, −1.72 to −2.41) correspond to the brain areas shown to be activated in rats (bregma, −2.3) with diabetes-induced neuropathic pain[28].

We used current-clamp recordings from cultured DRG neurons to characterize the direct effects of exogenous methylglyoxal on sensory neuron excitability (**Fig. 6**). Small- and medium-sized neurons from healthy WT and $Na_v1.8$ knockout mice did not differ in terms of resting membrane potential, current threshold and voltage threshold[29]. In the WT neurons, exposure to 100 µM methylglyoxal for 3 h resulted in a significant depolarizing shift by 8.2 mV in the resting membrane potential, a reduced current threshold for the activation of action potentials and a reduction in the depolarization required to reach the voltage threshold (**Fig. 6a**,**b**). The relative decrease in the current threshold in the WT neurons was larger (44%) than the decrease in voltage threshold (30%), which may indicate that the membrane resistance was increased by exposure to methylglyoxal. The rise time of the action potential was longer in WT methylglyoxal-treated (1.7 ms ± 0.1 ms (mean ± s.e.m)) than in control untreated WT neurons (1.3 ms ± 0.08 ms, $P < 0.01$), reflecting the lowered voltage threshold as a result of methylglyoxal treatment. Exposure of the WT neurons to a lower concentration of methylglyoxal (1 µM), corresponding to the plasma concentrations found in patients with diabetes and pain, for an extended period of time (12–14 h) also rendered their resting membrane potentials more depolarized (**Fig. 6c**; 4.3 mV, $P < 0.01$), however, their current and voltage thresholds were only reduced insignificantly. Additional pretreatment of these neurons with aminoguanidine, which inhibits protein modifications by methylglyoxal, was able to prevent the depolarizing effect of methylglyoxal, as well as the reduction of electrical thresholds (**Fig. 6c**).

Pretreatment of $Na_v1.8$ knockout neurons with methylglyoxal also resulted in a significant depolarizing shift by 5.2 mV of the resting membrane potential but did not induce a decrease in the current or voltage thresholds (**Fig. 6b**). Methylglyoxal pretreatment did not significantly change the amplitude or duration of either the

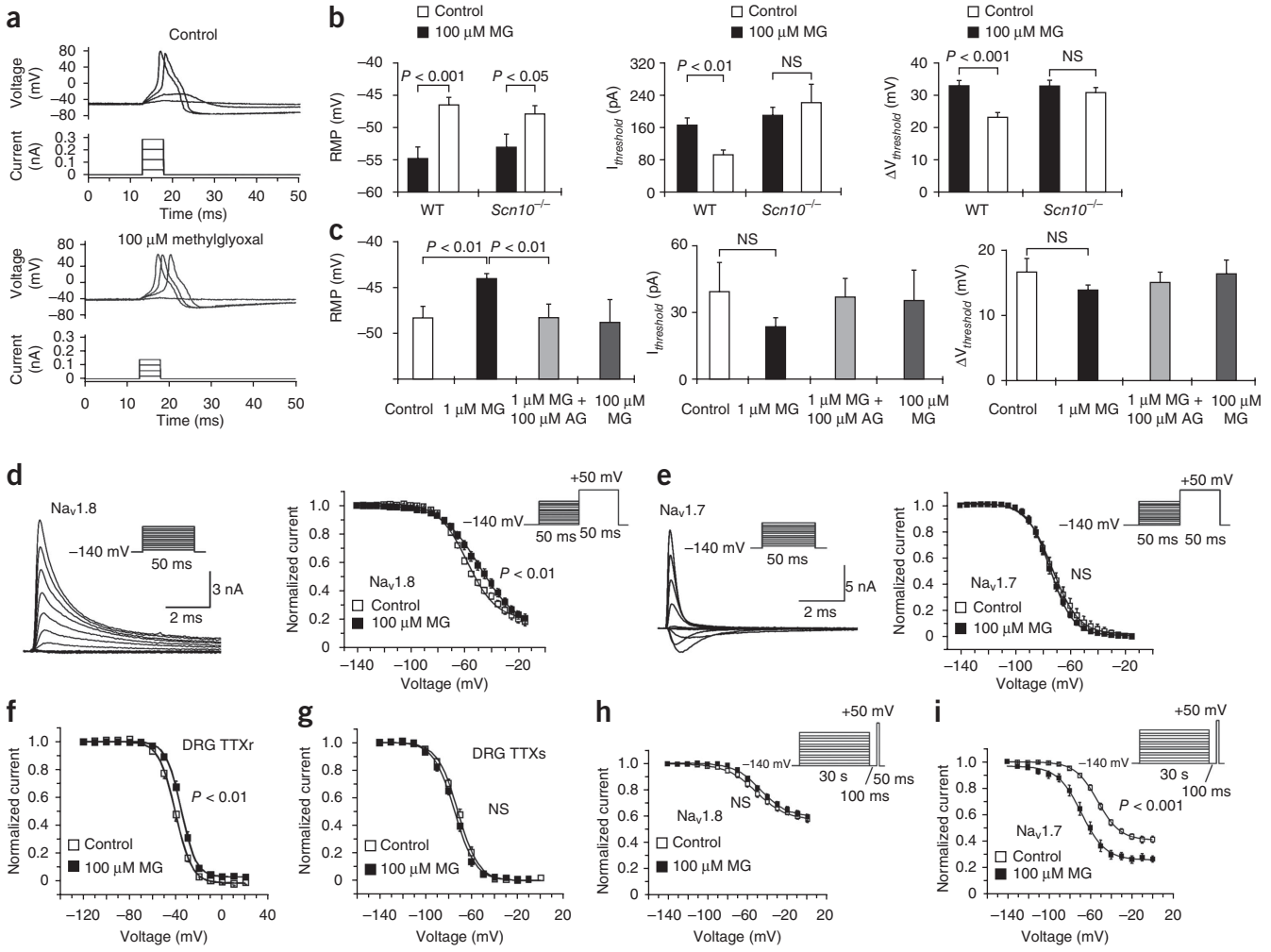

Figure 6 Effects of methylglyoxal on action potential generation and Na^+ currents in sensory neurons. (**a**) Examples of action potentials (upper traces) evoked by current pulses (lower traces) in neurons from WT mice stimulated with methylglyoxal. (**b**) The effect of methylglyoxal on the resting membrane potential, current threshold for pulses ($I_{threshold}$) and depolarization required to reach the threshold ($\Delta V_{threshold}$) in WT and $Na_v1.8$ knockout (*Scn10a*$^{-/-}$) neurons. Data represent the mean ± s.e.m. $n \geq 13$ neurons in each group. (**c**) The effects of methylglyoxal on the resting membrane potential, $I_{threshold}$ and $\Delta V_{threshold}$ in WT neurons in the presence and absence of aminoguanidine (AG). Data represent the mean ± s.e.m. $n \geq 13$ neurons per group. (**d**) A typical current trace of recombinant rat $Na_v1.8$ in ND7/23 cells activated by depolarizing steps (see insert) in the presence of TTX and voltage dependence of the steady-state fast inactivation of $Na_v1.8$ in ND7/23 cells (n = 12/12 (control/methylglyoxal treatment)). (**e**) A typical current trace of recombinant rat $Na_v1.7$ expressed in HEK293T cells, activated as shown in insert, but without any addition of TTX, showing the voltage dependence of the steady-state fast inactivation of $Na_v1.7$ (n = 13/14). NS, not significant. (**f**) The voltage dependence of the steady-state fast inactivation of TTXr Na^+ currents recorded in WT DRG neurons (n = 14/15). (**g**) The voltage dependence of the steady-state fast inactivation of TTXs currents recorded in $Na_v1.8$ knockout DRG neurons (n =11/11). (**h**) The voltage dependence of the steady-state slow inactivation of heterologously expressed $Na_v1.8$ (n = 12/10). (**i**) The voltage dependence of the steady-state slow inactivation of heterologously expressed $Na_v1.7$ expressed in HEK293T cells (n = 10/9). NS, not significant. All datasets shown in this figure were analyzed by two-tailed Student's unpaired t test.

action potential or the afterhyperpolarization in WT or $Na_v1.8$ knockout neurons (data not shown). These data suggest that biophysical changes in $Na_v1.8$ function are responsible for the methylglyoxal-induced hyperexcitability of sensory neurons but not for their depolarization.

We further assessed the effects of methylglyoxal pretreatment (3 h) using voltage clamp recordings on recombinant rat $Na_v1.8$ and $Na_v1.7$ in ND7/23 and HEK293T cells, respectively (**Fig. 6d**,**e** and **Supplementary Fig. 8**). We found methylglyoxal to have no effect on the voltage dependence of activation (data not shown). However, the midpoint of the steady-state fast inactivation of $Na_v1.8$ was significantly shifted toward more depolarized potentials (from $V_{0.5}$ = −58 mV ± 0.5 mV (mean ± s.e.m.) to $V_{0.5}$ = −48.7 mV ± 0.9 mV, n = 12), an effect that signifies increased channel availability at voltages corresponding to the action potential threshold (**Fig. 6d**). We did not find this effect on fast inactivation when we applied methylglyoxal only briefly (3 min) before beginning the test protocol (data not shown). This is compatible with the time required for post-translational protein modifications to occur and excludes rapid, non-specific membrane effects. Methylglyoxal did not shift the steady-state fast inactivation of $Na_v1.7$ (**Fig. 6e**).

To reproduce the differential effects of methylglyoxal on the steady-state fast inactivation of $Na_v1.8$ and $Na_v1.7$ (**Fig. 6d**,**e** and **Supplementary Fig. 8**), we performed identical experiments on native TTXr and tetrodotoxin-sensitive (TTXs) Na^+ currents, which are the executive action potential generators in nociceptive DRG neurons[26].

We conducted the experiments in cultured DRG neurons of WT mice in the presence of TTX to monitor the effects on $Na_v1.8$ and of $Na_v1.8$ knockouts to monitor the effects on $Na_v1.7$ and other TTXs subunits.

We found a small but significant methylglyoxal-induced shift in the midpoint (from $V_{0.5} = -41$ mV ± 0.2 mV to $V_{0.5} = -36$ mV ± 0.2 mV, $n = 15$ (control) or 14 (methylglyoxal treatment)) of the steady-state fast inactivation for the TTXr currents (**Fig. 6f**) but not for the TTXs currents (**Fig. 6g**). Thus, methylglyoxal increased the known relative resistance of the TTXr action potential generator against fast inactivation, which may have contributed to the increased excitability. Using the same heterologous expression systems as described above, we then studied slow steady-state inactivation using recombinant VGSC.Whereas this voltage-dependent function of $Na_v1.8$ was not influenced by pretreatment with methylglyoxal (**Fig. 6h**), we did observe a significant shift toward more hyperpolarized potentials (from $V_{0.5} = -53$ mV ± 0.8 mV to $V_{0.5} = -68$ mV ± 0.6 mV, $n = 10$ (methylglyoxal treatment) or 9 (control)) with $Na_v1.7$ as a result of methylglyoxal pretreatment (**Fig. 6i**), reducing the availability of the $Na_v1.7$ channels at the resting membrane potential by half. As $Na_v1.7$ is known to be crucial for action potential triggering in nociceptive neurons, the slow inactivation of these ion channels could account for the methylglyoxal-induced hypoalgesia observed in the $Na_v1.8$ knockout mice (**Fig. 4g**). The contrary effects of methylglyoxal on $Na_v1.8$ and $Na_v1.7$ functions (sensitization and inactivation, respectively) argues against an indirect action of methylglyoxal, for example, by inducing COX-2 expression, which might enhance prostaglandin formation[30]. Although this and other inflammatory mediators increase the voltage sensitivity of $Na_v1.8$, they are not known to enhance the slow inactivation of $Na_v1.7$ (refs. 19,25).

DISCUSSION

Our data support a new mechanistic concept of painful peripheral neuropathy in diabetes. Post-translational modification of the nociceptor-specific sodium channel $Na_v1.8$ by methylglyoxal is associated with enhanced sensory neuron excitability and hyperalgesia, whereas methylglyoxal slows myelinated nerve conduction and drives $Na_v1.7$ into slow inactivation. As crystallographic and site-directed mutagenesis studies on these VGSCs are not yet available, the exact molecular link between methylglyoxal and changes in channel function is unknown. Other modifications secondary to treatment with methylglyoxal cannot be excluded as being responsible for the functional changes observed, such as the depolarizing effect. However, the biochemical and functional data presented here support the hypothesis that methylglyoxal-dependent modification(s) in $Na_v1.8$ have a role in diabetes-associated hyperalgesia that is independent of degenerative or regenerative changes in the nerve.

The concentration of plasma methylglyoxal is increased in patients with diabetes as a result of increased formation of methylglyoxal from excessive glycolysis[4] and decreased degradation and detoxification by the glyoxalase system. Other pathological states resulting in increased concentrations of methylglyoxal are uremia and ischemia-reperfusion. Although symptoms of painful diabetic neuropathy arise spontaneously, such as burning and prickling sensations in the feet, tactile allodynia is a classical sign of this condition, and burning pain can be provoked by warming the patients' feet[31]. Thus, the thermal and mechanical hypersensitivity in diabetic, healthy methylglyoxal-injected or GLO1-deficient mice can be considered to reflect, at least in part, the human symptoms.

To the best of our knowledge, methylglyoxal is the first endogenously produced small molecule (as opposed to cytokines, some of which induce systemic hyperalgesia) that induces thermal and mechanical hyperalgesia in healthy mice by acute systemic administration. Systemic application of methylglyoxal, however, gave rise to some ambiguity as to the target of its post-translational modification. CGRP release experiments, however, confirmed the induction of peripheral hypersensitivity by methylglyoxal and the dependence of this induction on $Na_v1.8$ expression. In diabetic neuropathy, the axonal transport of neuropeptide-containing dense core vesicles is impeded, which leads to reduced basal release from the skin nerve endings. However, stimulated neurosecretion is facilitated in diabetic neuropathy, suggesting an increased sensitivity, excitability or both[32]. These findings in the skin do not exclude additional effects of methylglyoxal on the nonpeptidergic subpopulation of nociceptors or on spinal terminals where further sensitization of synaptic transmission could occur[33].

The altered function of $Na_v1.8$ (reduced inactivation, as well as increased whole-cell excitability) is consistent with methylglyoxal binding to TTXr sodium channels and with the lack of methylglyoxal-induced hyperalgesia in $Na_v1.8$ knockout mice and siRNA-treated healthy WT mice. The prominent methylglyoxal-induced neuronal depolarization and the concomitant increase in membrane resistance both increase the chance for sensory functions, for example, heat-induced generator potentials or accidental spontaneous depolarization, to reach the relatively high voltage threshold of $Na_v1.8$ and generate action potentials[34]. Notably, methylglyoxal also causes a major slow inactivation of $Na_v1.7$, an essential VGSC and 'threshold channel' in nociceptive neurons. This inactivation of the TTXs sodium channel would be aggravated *in vivo* by the methylglyoxal-induced depolarization, and only unmyelinated nerve fibers, which have a high abundance of the inactivation-resistant $Na_v1.8$ in their endings, are expected to show increased excitability. In fact, the partial block of $Na_v1.7$ by methylglyoxal may explain why $Na_v1.8$ knockout mice show hypoalgesia in response to methylglyoxal, as hardly any action potential generator would be left in the nociceptors under these conditions. Similarly, postganglionic neurons of the autonomic nervous system, which are often affected by diabetic neuropathy and express $Na_v1.7$ but not $Na_v1.8$ (refs. 33,34), would fail under the condition of accumulating methylglyoxal. These opposing effects of methylglyoxal on TTXs compared to TTXr VGSCs could account for the coexistence of positive and negative clinical symptoms, such as burning feet and diabetic gastroparesis. Support for the general impairment of TTXs sodium channels by methylglyoxal comes from the marked slowing of NCV after systemic methylglyoxal administration.

Nociceptive neurons that express $Na_v1.8$ in their peripheral terminals gain one more 'profit' from the modifying actions of methylglyoxal, as $Na_v1.8$ is a faster repriming action potential generator than $Na_v1.7$ (ref. 18). Thus, the discharge rate in response to a given depolarization of the affected neuron can rise when the trigger function for discharge passes from the inactivated $Na_v1.7$ to the facilitated $Na_v1.8$. Modification of $Na_v1.8$ by methylglyoxal seems to be the root of primary hyperalgesia in animals, as well as the cause of pain in patients with diabetes. Although short-term diabetes in mice is not comparable to years of diabetes in humans, our findings suggest that methylglyoxal is a valid therapeutic target for the treatment of painful diabetic neuropathy, a medical condition for which few effective therapeutic options are available.

METHODS

Methods and any associated references are available in the online version of the paper.

Note: Supplementary information is available in the online version of the paper.

ACKNOWLEDGMENTS

The authors thank S. Kaymak for immunohistochemistry, A. Buhl and K. Leotta for assistance in the cerebral blood flow experiments, L. Werner for support with bregma gradings and X. Du and A. Erhardt for the daily care of the mice. A. Bierhaus, J.F., M.E.C., M.B. and P.P.N. were supported by a Centre grant from the Juvenile Diabetes Research Foundation (JDRF). This work was also supported in part by grants from the Deutsche Forschungsgemeinschaft (BI-1281/3-1 to A. Bierhaus; LU728/3-1 and NA-350/3-2 in KFO 130 to P.W.R., C. Nau and A.L.), the US National Institutes of Health (2R56DK33861-21 to M.B.), the European Foundation for the Study of Diabetes (EFSD/Lilly-Programme, to A. Bierhaus), the German Diabetes Association (DDG, Christian-Hagedorn-Award to A. Bierhaus), the Manfred-Lautenschläger-Stiftung for Diabetes (LSD, to P.P.N.), the Dietmar-Hopp-Stiftung (to A. Bierhaus, P.M.H. and P.P.N.) and the Network Aging Research (NAR, to A. Bierhaus). A. Babes and C.N. were supported by grant PN2 164/2007 from the Romanian Research Council (CNCSIS). A. Babes also received support from the Alexander von Humboldt Foundation.

AUTHOR CONTRIBUTIONS

A. Bierhaus planned, performed and supervised all experiments, was responsible for the data interpretation and wrote the manuscript. T.F. and S.S. performed most of the mouse experiments, and T.F. also did the biochemical analytics and cell culture experiments. A.L. and C. Nau performed the voltage clamp studies and were involved in data interpretation. A. Babes and C. Neacsu performed the current clamp studies and were involved in data interpretation. S.K.S., M.E. and T.I.K. performed CGRP-release experiments and single-fiber recordings in the skin-nerve preparation and were involved in data interpretation. M. Schnölzer, N.R. and P.J.T. were involved in the dicarbonyl analytics and data interpretation. F.L. provided biopsies of human sciatic nerves. W.L.N. performed electron microscopy. R.E. and I.K.L. performed the nerve conduction velocity experiments and the measurements of tactile allodynia. W.M., M. Schwaninger and U.H. supervised the cerebral blood flow measurements and were involved in data interpretation. T.D. was involved in the isolation and characterization of the DRG. D.E. generated the *Glo1*$^{-/+}$ mice. J.F. and M.E.C. provided ALT-711 and were involved in data interpretation. I.K., V.P. and M.M. performed the clinical studies. P.M.H. supervised the clinical studies and was involved in data interpretation. D.M.S. was involved in data interpretation and the writing of the manuscript. D.Z. provided the human skin biopsies and was involved in data interpretation. M.B. provided the *Glo1*$^{-/+}$ mice and was involved in data interpretation and the writing of the manuscript. P.W.R. supervised the electrophysiological part of the project and wrote the manuscript. P.P.N. supervised the project and wrote the manuscript. Senior coauthorship is shared by P.W.R. and P.P.N.

COMPETING FINANCIAL INTERESTS

The authors declare no competing financial interests.

Published online at http://www.nature.com/doifinder/10.1038/nm.2750.
Reprints and permissions information is available online at http://www.nature.com/reprints/index.html.

1. Tavee, J. & Zhou, L. Small fiber neuropathy: a burning problem. *Cleve. Clin. J. Med.* **76**, 297–305 (2009).
2. Nawroth, P.P., Rudofsky, G. & Humpert, P.M. Have we understood diabetes? New tasks for diagnosis and therapy. *Exp. Clin. Endocrinol. Diabetes* **118**, 1–3 (2010).
3. Calcutt, N.A. Potential mechanisms of neuropathic pain in diabetes. *Int. Rev. Neurobiol.* **50**, 205–228 (2002).
4. Thornalley, P.J. Dicarbonyl intermediates in the maillard reaction. *Ann. NY Acad. Sci.* **1043**, 111–117 (2005).
5. Brownlee, M. Biochemistry and molecular cell biology of diabetic complications. *Nature* **414**, 813–820 (2001).
6. Karachalias, N., Babaei-Jadidi, R., Ahmed, N. & Thornalley, P.J. Accumulation of fructosyl-lysine and advanced glycation end products in the kidney, retina and peripheral nerve of streptozotocin-induced diabetic rats. *Biochem. Soc. Trans.* **31**, 1423–1425 (2003).
7. Thornalley, P.J. Glyoxalase I—structure, function and a critical role in the enzymatic defence against glycation. *Biochem. Soc. Trans.* **31**, 1343–1348 (2003).
8. Bierhaus, A. & Nawroth, P.P. Multiple levels of regulation determine the role of the receptor for AGE (RAGE) as common soil in inflammation, immune responses and diabetes mellitus and its complications. *Diabetologia* **52**, 2251–2263 (2009).
9. Jack, M.M., Ryals, J.M. & Wright, D.E. Characterisation of glyoxalase I in a streptozocin-induced mouse model of diabetes with painful and insensate neuropathy. *Diabetologia* **54**, 2174–2182 (2011).
10. Morcos, M. *et al.* Glyoxalase-1 prevents mitochondrial protein modification and enhances lifespan in *Caenorhabditis elegans*. *Aging Cell* **7**, 260–269 (2008).
11. Suzuki, Y., Sato, J., Kawanishi, M. & Mizumura, K. Lowered response threshold and increased responsiveness to mechanical stimulation of cutaneous nociceptive fibers in streptozotocin-diabetic rat skin *in vitro*—correlates of mechanical allodynia and hyperalgesia observed in the early stage of diabetes. *Neurosci. Res.* **43**, 171–178 (2002).
12. Misawa, S. *et al.* Axonal potassium conductance and glycemic control in human diabetic nerves. *Clin. Neurophysiol.* **116**, 1181–1187 (2005).
13. Grafe, P., Bostock, H. & Schneider, U. The effects of hyperglycaemic hypoxia on rectification in rat dorsal root axons. *J. Physiol. (Lond.)* **480**, 297–307 (1994).
14. Quasthoff, S. The role of axonal ion conductances in diabetic neuropathy: a review. *Muscle Nerve* **21**, 1246–1255 (1998).
15. Craner, M.J., Klein, J.P., Renganathan, M., Black, J.A. & Waxman, S.G. Changes of sodium channel expression in experimental painful diabetic neuropathy. *Ann. Neurol.* **52**, 786–792 (2002).
16. Hong, S., Morrow, T.J., Paulson, P.E., Isom, L.L. & Wiley, J.W. Early painful diabetic neuropathy is associated with differential changes in tetrodotoxin-sensitive and -resistant sodium channels in dorsal root ganglion neurons in the rat. *J. Biol. Chem.* **279**, 29341–29350 (2004).
17. Shah, B.S. *et al.* Beta3, a novel auxiliary subunit for the voltage gated sodium channel is upregulated in sensory neurones following streptozocin induced diabetic neuropathy in rat. *Neurosci. Lett.* **309**, 1–4 (2001).
18. Lampert, A., O'Reilly, A.O., Reeh, P. & Leffler, A. Sodium channelopathies and pain. *Pflugers Arch.* **460**, 249–263 (2010).
19. Silos-Santiago, I. The role of tetrodotoxin-resistant sodium channels in pain states: are they the next target for analgesic drugs? *Curr. Opin. Investig. Drugs* **9**, 83–89 (2008).
20. Hirade, M., Yasuda, H., Omatsu-Kanbe, M., Kikkawa, R. & Kitasato, H. Tetrodotoxin-resistant sodium channels of dorsal root ganglion neurons are readily activated in diabetic rats. *Neuroscience* **90**, 933–939 (1999).
21. Konrade, I. *et al.* Verminderte glyoxalase-1 aktivitat bei patienten mit schmerzhafter diabetischer neuropathie. *Diabetologie und Stoffwechsel* **2**, P98 (2007).
22. Thornalley, P.J. *et al.* Antitumour activity of S-p-bromobenzylglutathione cyclopentyl diester *in vitro* and *in vivo*. Inhibition of glyoxalase I and induction of apoptosis. *Biochem. Pharmacol.* **51**, 1365–1372 (1996).
23. El-Osta, A. *et al.* Transient high glucose causes persistent epigenetic changes and altered gene expression during subsequent normoglycemia. *J. Exp. Med.* **205**, 2409–2417 (2008).
24. Sullivan, K.A. *et al.* Mouse models of diabetic neuropathy. *Neurobiol. Dis.* **28**, 276–285 (2007).
25. Kellogg, A.P., Cheng, H.T. & Pop-Busui, R. Cyclooxygenase-2 pathway as a potential therapeutic target in diabetic peripheral neuropathy. *Curr. Drug Targets* **9**, 68–76 (2008).
26. Hong, S., Agresta, L., Guo, C. & Wiley, J.W. The TRPV1 receptor is associated with preferential stress in large dorsal root ganglion neurons in early diabetic sensory neuropathy. *J. Neurochem.* **105**, 1212–1222 (2008).
27. Morrow, T.J., Paulson, P.E., Danneman, P.J. & Casey, K.L. Regional changes in forebrain activation during the early and late phase of formalin nociception: analysis using cerebral blood flow in the rat. *Pain* **75**, 355–365 (1998).
28. Paulson, P.E., Wiley, J.W. & Morrow, T.J. Concurrent activation of the somatosensory forebrain and deactivation of periaqueductal gray associated with diabetes-induced neuropathic pain. *Exp. Neurol.* **208**, 305–313 (2007).
29. Renganathan, M., Cummins, T.R. & Waxman, S.G. Contribution of $Na_V1.8$ sodium channels to action potential electrogenesis in DRG neurons. *J. Neurophysiol.* **86**, 629–640 (2001).
30. Fuchs, D., Birklein, F., Reeh, P.W. & Sauer, S.K. Sensitized peripheral nociception in experimental diabetes of the rat. *Pain* **151**, 496–505 (2010).
31. Obrosova, I.G. Diabetic painful and insensate neuropathy: pathogenesis and potential treatments. *Neurotherapeutics* **6**, 638–647 (2009).
32. Sandkühler, J. Models and mechanisms of hyperalgesia and allodynia. *Physiol. Rev.* **89**, 707–758 (2009).
33. Rush, A.M., Cummins, T.R. & Waxman, S.G. Multiple sodium channels and their roles in electrogenesis within dorsal root ganglion neurons. *J. Physiol. (Lond.)* **579**, 1–14 (2007).
34. Rush, A.M. *et al.* A single sodium channel mutation produces hyper- or hypoexcitability in different types of neurons. *Proc. Natl. Acad. Sci. USA* **103**, 8245–8250 (2006).
35. Ahmed, N., Dobler, D., Dean, M. & Thornalley, P.J. Peptide mapping identifies hotspot site of modification in human serum albumin by methylglyoxal involved in ligand binding and esterase activity. *J. Biol. Chem.* **280**, 5724–5732 (2005).

ONLINE METHODS

Mouse and cell culture models. *Glo1*$^{-/+}$ and $Na_v1.8$ knockout (*Scn10*$^{-/-}$) mice are viable and have normal reproductive function. All strains were backcrossed on the C57BL/6 background more than ten times, and C57BL/6 mice served as controls for all transgenic mice. BKS db/db mice (BKS.Cg-m$^{+/+}$Lprdb/Bom Tac) and the respective control littermates were purchased from Taconic (Lille Skensved, Denmark). Mice were housed individually with a 12-hour, 12-hour light, dark cycle and were given free access to food and water. All procedures in this study were approved by the Animal Care and Use Committees at the Regierungspräsidium Tübingen and Karlsruhe, Germany (35-9185.81/G-90/04 and 35-9185.81/G-182/08). Diabetes was induced in mice by intraperitoneal administration of STZ, and diabetes was maintained over a period of 8 weeks by monitoring of blood glucose. Rat $Na_v1.8$ and $Na_v1.7$ complementary DNA was transiently transfected in the dorsal root ganglion neuroblastoma hybridoma cell line ND7/23 or the human embryonic kidney cell line HEK283T, respectively.

Measurements of hyperalgesia. Thermal and tactile hyperalgesia were determined following the standard protocols for the Hot Plate, Hargreaves, Tail Flick and Von Frey filament assays[36–40]. Repetitive *in vivo* determination of NCV was performed as described previously[41]. Neuronal activation in selected brain regions was determined by autoradiographic measurement of regional CBF[42].

***In vivo* treatments.** GLO1 activity was modulated either by *in vivo* overexpression of GLO1 using somatic gene transfer[43] or using the GLO1 inhibitor S-p-bromobenzylglutathione cyclopentyl diester[22]. Where indicated, predesigned siRNA for the mouse voltage-gated sodium channels $Na_v1.7$ (*Scn9A*), $Na_v1.8$ (*Scn10a*) and TRPV1 and the respective control siRNAs were administered in liposomal transfection reagent by intravenous injection. The synthetic methylglyoxal-scavenging peptide $GERP_{10}$ (United States Letters patent number 61/182203, May 29, 2009) was injected once intraperitoneally at a concentration of 1 mg per mouse.

Electrophysiological recordings. Neurons were used for current clamp and voltage clamp recordings within 2 d of dissection following the protocols listed in the **Supplementary Methods**. Slow inactivation was induced by 30-s prepulses ranging from −140 mV to 0 mV in steps of 10 mV. Test pulses to +50 mV were applied after a 100-ms long interpulse at −140 mV, which allowed for recovery from fast inactivation (see inserts in **Fig. 6**).

Biochemistry and RNA and protein processing. DRGs and tissue for the biochemical analysis, immunoprecipitation, western blot or PCR were prepared and analyzed as previously described[44,45]. The primers used for real-time PCR are provided in **Supplementary Table 2**. Plasma methylglyoxal concentrations were determined by HPLC, and GLO1 activity was measured spectrophotometrically.

Patient samples. All patient samples used were from a previously described cohort[46], and patient characteristics are provided in **Supplementary Table 1**. Human sciatic nerves were received from the Gewebebank für Entzündliche Erkrankungen (GEZEH) of the University of Heidelberg (http://www.gezeh.de). The study protocol was approved by the University of Heidelberg Ethics Committee, and all patients gave written informed consent at the time of hospitalization.

Statistics. All data are expressed as mean values ± s.d. ($n \leq 5$) or mean values ± s.e.m. ($n \geq 10$). In all functional, biochemical and molecular assays in mice (not electrophysiological assays), measurements were performed in groups with equal numbers; either $N = 5$ or 10 per group. Unpaired, two-tailed Student's *t* test was used to compare data within one experimental group, and ANOVA followed by least significant difference *post hoc* analysis was used for comparison of different experimental groups. Statistical analyses were performed using SPSS software version 15.0 (SPSS Inc., Chicago, USA). Any $P > 0.05$ was considered to be statistically insignificant.

Additional methods. A detailed description of all methods and reagents used throughout the manuscript are provided in the **Supplementary Methods**.

36. Bierhaus, A. *et al.* Loss of pain perception in diabetes is dependent on a receptor of the immunoglobulin superfamily. *J. Clin. Invest.* **114**, 1741–1751 (2004).
37. Menéndez, L., Lastra, A., Hidalgo, A. & Baamonde, A. Unilateral hot plate test: a simple and sensitive method for detecting central and peripheral hyperalgesia in mice. *J. Neurosci. Methods* **113**, 91–97 (2002).
38. Hargreaves, K., Dubner, R., Brown, F., Flores, C. & Joris, J. A new and sensitive method for measuring thermal nociception in cutaneous hyperalgesia. *Pain* **32**, 77–88 (1988).
39. D'Amour, F.E., Erickson, B.R. & Smith, D.L. Effect of environmental temperature in traumatic shock. *Proc. Soc. Exp. Biol. Med.* **94**, 1–4 (1957).
40. Vareniuk, I., Pavlov, I.A. & Obrosova, I.G. Inducible nitric oxide synthase gene deficiency counteracts multiple manifestations of peripheral neuropathy in a streptozotocin-induced mouse model of diabetes. *Diabetologia* **51**, 2126–2133 (2008).
41. Miyoshi, T. & Goto, I. Serial *in vivo* determinations of nerve conduction velocity in rat tails. Physiological and pathological changes. *Electroencephalogr. Clin. Neurophysiol.* **35**, 125–131 (1973).
42. Morrow, T.J., Paulson, P.E., Brewer, K.L., Yezierski, R.P. & Casey, K.L. Chronic, selective forebrain responses to excitotoxic dorsal horn injury. *Exp. Neurol.* **161**, 220–226 (2000).
43. Zhang, Y. *et al.* Intravenous somatic gene transfer with antisense tissue factor restores blood flow by reducing tumor necrosis factor-induced tissue factor expression and fibrin deposition in mouse meth-A sarcoma. *J. Clin. Invest.* **97**, 2213–2224 (1996).
44. Stucky, C.L. & Lewin, G.R. Isolectin B(4)-positive and -negative nociceptors are functionally distinct. *J. Neurosci.* **19**, 6497–6505 (1999).
45. Bierhaus, A. *et al.* Diabetes-associated sustained activation of the transcription factor nuclear factor-κB. *Diabetes.* **50**, 2792–2808 (2001).
46. Humpert, P.M. *et al.* External electric muscle stimulation improves burning sensations and sleeping disturbances in patients with type 2 diabetes and symptomatic neuropathy. *Pain Med.* **10**, 413–419 (2009).

doi:10.1038\nm. 2750